I&EC research
Industrial & Engineering Chemistry Research
pubs.acs.org/IECR
Article

Continuous and Selective Separation of Heavy Metals Using Shock Electrodialysis

Mohammad A. Alkhadra and Martin Z. Bazant*

Cite This: https://doi.org/10.1021/acs.iecr.2c02627
Read Online
ACCESS | Metrics & More | Article Recommendations

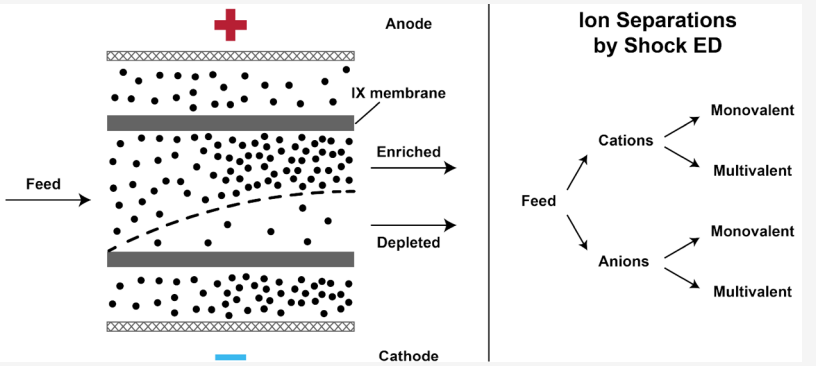

ABSTRACT: Selective separation of chemically and physically similar heavy metals is an important capability in extractive metallurgy and minerals processing. Metals with complex water chemistries present a fundamental challenge for selective hydrometallurgy, which often necessitates the implementation of complicated, many-step, and reagent-intensive processing techniques to achieve these separations. In this article, we use shock electrodialysis to continuously and selectively separate heavy metals, including cobalt, nickel, vanadium, molybdenum, and tungsten, from a synthetic leach liquor in a two-step process. In the first step, cobalt and nickel are separated from the other metals by selectively enriching these multivalent cations in the catholyte. In the second step, vanadium, molybdenum, and tungsten are separated from one another by adjusting the feed pH in the range of two to six to control the speciation of these metals. Our results demonstrate for the first time the utility of speciation control for selective ion separations by deionization shock waves.

INTRODUCTION

Heavy metals are characterized as metallic elements of relatively high density or atomic weight.[1] Most heavy metals also have the capacity to exist as ions in different oxidation states, as these species can readily lose or gain electrons in their partially filled d or f atomic orbitals. In solution, many heavy metals form water-stable cations, though the majority of simple, water-stable ions formed by the heavier d-block elements is oxyanions.[2] Vanadium, molybdenum, and tungsten are examples of heavy metals with many oxidation states that form extensive families of oxyanions in water. These species are used in many modern technologies and have a wide range of uses in alloy and steel manufacturing, catalysis, and electronics. Since primary resources of vanadium, molybdenum, and tungsten are insufficient to meet demand in the manufacture of advanced materials, extraction of these metals from secondary resources, such as ores (e.g., nickel−molybdenum ores) and spent catalysts (e.g., molybdenum−vanadium mixed oxides), has become increasingly important.[3] Moreover, efficient recovery of critical minerals in spent catalysts has great economic benefits, and it abates the environmental pollution associated with the disposal of these materials.[4−6] Many physical and metallurgical processes have been reported in the literature for separation and recovery of these elements, along with other valuable metals, from ores and spent catalysts.[3,7−9] In general, pyrometallurgy produces hazardous gases and leads to large losses of the metals, and biometallurgy requires complex process designs and high maintenance costs.[9] Hydrometallurgy, including precipitation,[10,11] adsorption,[12,13] ion exchange,[14,15] and solvent extraction,[3,16−21] is therefore widely used for the recovery of metals from various resources, typically after roasting and leaching the spent catalysts or ores.[3,7]

Received: July 22, 2022
Revised: September 30, 2022
Accepted: October 3, 2022

Since vanadium, molybdenum, and tungsten have similar chemical properties, the extraction and separation of these metals is difficult. In the literature, solvent extraction is often regarded as the best method for recovery of these metals from leach liquors.[3,8,9] However, solvent extraction exhibits low yields, requires large amounts of toxic organic solvents, and operates over long extraction times. Ion exchange is another common method for separation of heavy metals, though it requires use of specialty ion exchange resins and consumes larges volumes of concentrated acids and bases. In this paper, we adapt the emerging chemical-free method known as shock electrodialysis (or shock ED)[22−28] to electrokinetically separate vanadium, molybdenum, and tungsten. Shock ED has previously been used to remove toxic metal contaminants (usually multivalent cations) from water by transporting these species across a cation exchange membrane into the catholyte (see Figure 1).[27] Here, we demonstrate for the first time that

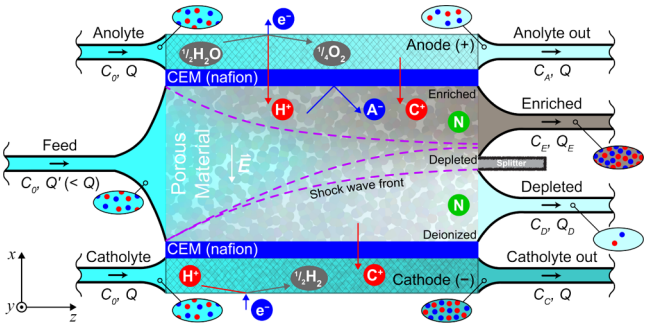

Figure 1. Schematic of the governing principles of shock ED. A rectangular cross section of the device shows water splitting at the anode and formation of molecular hydrogen at the cathode (maintained under acidic conditions), which are the primary electrochemical reactions that provide current to the cell. The feed is then subjected to an electric field ($\vec{E}$) that transports charged species (labeled C^+ for cations and A^- for anions) perpendicular to the flow. Anions are blocked by cation exchange membranes, and neutral species (labeled N) are unaffected by the electric field. For each stream, the flow rate is denoted by the letter Q, and concentration is denoted by the letter C; streams are colored based on the relative concentration of ions.

dissolved oxyanions can be continuously fractionated based on electric charge into two product streams without the need for these species to pass though an ion exchange membrane. In fact, fractionation can be achieved as long as an overlimiting current[27,29] is sustained across the device via the transport of a mobile cation (e.g., sodium, hydronium) through an ion selective surface (e.g., cation exchange membrane,[22,30] metal electrodeposit[31,32]). Our results reinforce the fact that separation of differently charged ions by shock ED relies on the action of a deionization shock wave (i.e., a sharp concentration gradient) in weakly charged porous media.[27,30,33] As shown in Figure 1, the deionization shock splits the feed of dissolved metals into two product streams, which are continuously separated by driving a flow perpendicular to the applied electric field.[22,34,35]

MATERIALS AND EXPERIMENTAL METHODS

Thermodynamic Simulation of Chemical Equilibria. The distribution diagrams shown in Figure 2 were generated for the concentrations in Table 2 and at 25 °C using the open-source thermodynamics software DATABASE and graphical

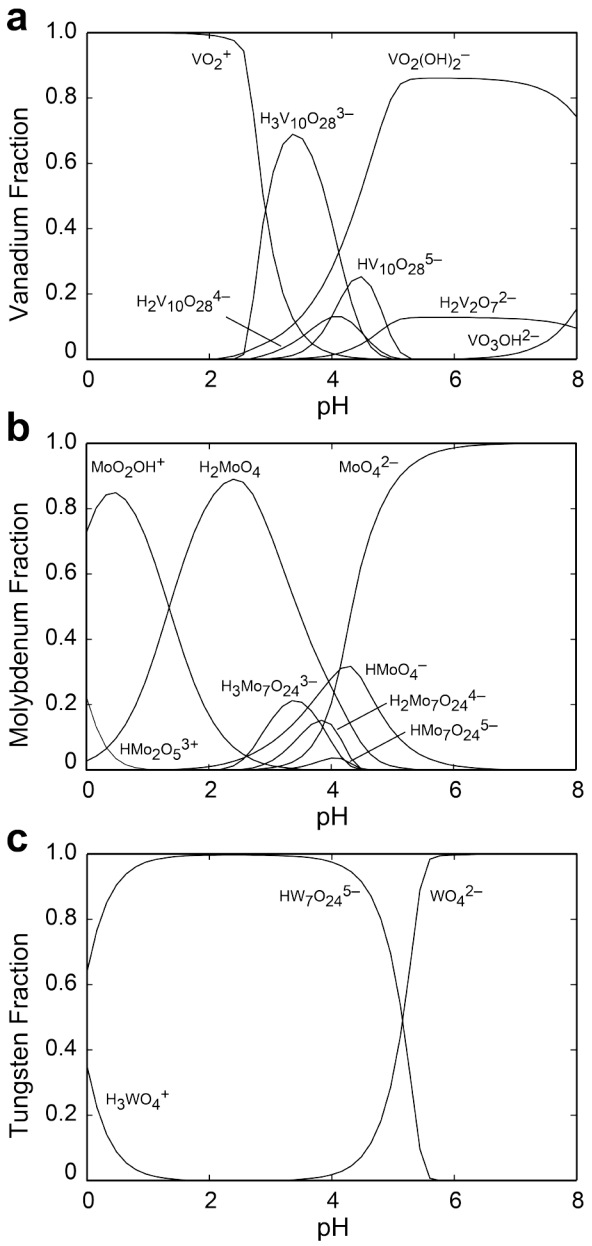

Figure 2. Distribution diagrams of (a) vanadium, (b) molybdenum, and (c) tungsten versus pH for the concentrations in Table 2 and at 25 °C. These data were obtained using the open-source thermodynamics software DATABASE. Ionic strength was calculated in these simulations, and the chemical reactions and equilibrium constants of all species considered in the simulations are reported in Table 1.

user interface SPANA. The chemical reactions and equilibrium constants of all species considered in the simulations are preloaded in the DATABASE package and reproduced in Table 1. (The parameters in DATABASE are obtained from the NIST Critically Selected Stability Constants of Metal Complexes database[36] and other sources.[37,38]) This program solves the mass balance equations for the components in an aqueous mixture using these chemical reactions and equilibrium constants.

Device Design and Fabrication. The device used here, shown schematically in Figure 1, is based on a design previously published by our group.[23,26,28] The device consists

https://doi.org/10.1021/acs.iecr.2c02627
Ind. Eng. Chem. Res. XXXX, XXX, XXX−XXX

Table 1. Chemical Reactions and Equilibrium Constants at 25 °C Used in Thermodynamic Simulations to Produce Elemental Distribution Diagrams

chemical reaction	equilibrium constant, log K
$H^+ + VO(OH)_3 \rightleftharpoons VO_2^+ + 2H_2O$	4.2
$2H^+ + VO_2(OH)_2^- \rightleftharpoons VO_2^+ + 2H_2O$	6.8
$3H^+ + VO_3OH^{2-} \rightleftharpoons VO_2^+ + 2H_2O$	15.6
$4H^+ + VO_4^{3-} \rightleftharpoons VO_2^+ + 2H_2O$	29.5
$4H^+ + H_2V_2O_7^{2-} \rightleftharpoons 2VO_2^+ + 3H_2O$	11.3
$5H^+ + HV_2O_7^{3-} \rightleftharpoons 2VO_2^+ + 3H_2O$	20.9
$6H^+ + V_2O_7^{4-} \rightleftharpoons 2VO_2^+ + 3H_2O$	32.2
$8H^+ + V_4O_{12}^{4-} \rightleftharpoons 4VO_2^+ + 4H_2O$	19.6
$13H^+ + H_3V_{10}O_{28}^{3-} \rightleftharpoons 10VO_2^+ + 8H_2O$	5.1
$14H^+ + H_2V_{10}O_{28}^{4-} \rightleftharpoons 10VO_2^+ + 8H_2O$	9.8
$15H^+ + HV_{10}O_{28}^{5-} \rightleftharpoons 10VO_2^+ + 8H_2O$	14.0
$16H^+ + V_{10}O_{28}^{6-} \rightleftharpoons 10VO_2^+ + 8H_2O$	21.5
$H^+ + MoO_4^{2-} \rightleftharpoons HMoO_4^-$	4.2
$2H^+ + MoO_4^{2-} \rightleftharpoons H_2MoO_4$	8.2
$3H^+ + MoO_4^{2-} \rightleftharpoons H_2O + MoO_2OH^+$	9.5
$5H^+ + 2\,MoO_4^{2-} \rightleftharpoons 2H_2O + Mo_2O_5OH^+$	18.8
$6H^+ + 2\,MoO_4^{2-} \rightleftharpoons 3H_2O + Mo_2O_5^{2+}$	20.3
$7H^+ + 2\,MoO_4^{2-} \rightleftharpoons 3H_2O + HMo_2O_5^{3+}$	20.1
$8H^+ + 7\,MoO_4^{2-} \rightleftharpoons 4H_2O + Mo_7O_{24}^{6-}$	54.3
$9H^+ + 7\,MoO_4^{2-} \rightleftharpoons 4H_2O + HMo_7O_{24}^{5-}$	60.7
$10H^+ + 7\,MoO_4^{2-} \rightleftharpoons 4H_2O + H_2Mo_7O_{24}^{4-}$	65.5
$11H^+ + 7\,MoO_4^{2-} \rightleftharpoons 4H_2O + H_3Mo_7O_{24}^{3-}$	69.5
$H^+ + WO_4^{2-} \rightleftharpoons HWO_4^-$	3.6
$2H^+ + WO_4^{2-} \rightleftharpoons H_2WO_4$	5.8
$3H^+ + WO_4^{2-} \rightleftharpoons H_3WO_4^+$	7.2
$6H^+ + 6WO_4^{2-} \rightleftharpoons 3H_2O + W_6O_{21}^{6-}$	47.0
$8H^+ + 7WO_4^{2-} \rightleftharpoons 4H_2O + W_7O_{24}^{6-}$	54.1
$9H^+ + 7WO_4^{2-} \rightleftharpoons 4H_2O + HW_7O_{24}^{5-}$	71.3
$14H^+ + 12WO_4^{2-} \rightleftharpoons 7H_2O + W_{12}O_{41}^{10-}$	105.7
$H_2O \rightleftharpoons H^+ + OH^-$	−14.0

of three inlets (two to transport the electrode streams and a third to deliver the feed) and four outlets (two to transport the electrode streams and two to generate depleted and enriched product streams at the splitter). All fluids are transported through 1/8th-inch Tygon tubing (Saint-Gobain) glued onto portplates made of cast acrylic. These portplates seal liquids inside the device and support the rubber tubing through which fluid flows. Moreover, four 1/16th-inch Viton rubber gaskets (DuPont) are used to seal the device and simultaneously provide channels for the electrode streams. The electrodes are made of platinum meshes (Sigma−Aldrich), which are connected to a Gamry Reference 3000 potentiostat/galvanostat using titanium wires (Alfa Aesar). The electrodes and wires are secured in place by compressible Viton gaskets. Cation exchange membranes (Nafion N115, Ion Power) with a thickness of approximately 130 μm and an area of 1.0 cm^2 are used as fluidic barriers between the electrode channels and the porous material.

The porous material is a borosilicate frit (Adams & Chittenden Scientific Glass) with ultrafine pores (nominally ranging from 0.9 to 1.4 μm in size), an internal surface area of 1.75 $m^2\ g^{-1}$ based on Brunauer−Emmett−Teller theory, a mass density of 1.02 g m^{-3}, a porosity of 0.31, and approximate dimensions of 0.5 cm × 1.8 cm × 0.6 cm ($x \times y \times z$). The frit is glued onto acrylic frames using Devcon 2 Ton Epoxy (McMaster-Carr). The splitter (placed midway down the outlet for ease of assembly) is made of cast acrylic and sealed against the top face of the porous material using 0.04-in. GORE expanded polytetrafluoroethylene (PTFE) gasket tape. During assembly, holes in all of the acrylic slabs and rubber gaskets are formed using a laser cutter (Universal Laser Systems) and refined with a drill press (Palmgren ten-inch, five-speed bench model). These layers are then stacked and held together with nuts, bolts, and washers made of 316 stainless steel.

Preparation of Feed and Electrode Solutions. In previous work by our group, we demonstrated the ability of shock ED with a borosilicate frit to selectively separate multivalent ions in the presence of excess competing sodium,[24,26] and we proposed several possible mechanisms of this selectivity in a theoretical study.[39] To simplify the processing and analysis of samples in this study and to isolate the role of speciation control on selectivity, we use a synthetic mixture in which all dissolved metals are present in approximately equal proportions, as shown in Table 2. This solution is prepared by first formulating stock solutions with concentrations of 1000 mg L^{-1} made from sodium orthovanadate (Na_3VO_4), sodium molybdate (Na_2MoO_4), and sodium tungstate dihydrate ($Na_2WO_4{\cdot}2H_2O$). We also formulated stock solutions with concentrations of 1000 mg L^{-1} made from cobalt sulfate heptahydrate ($CoSO_4{\cdot}7H_2O$) and nickel sulfate heptahydrate ($NiSO_4{\cdot}7H_2O$) to prepare the synthetic leach liquor. Appropriate volumes of these solutions were then diluted in deionized water, and the pH of these mixtures was adjusted using hydrochloric acid (HCl). All reagents were obtained from Sigma−Aldrich. The anolyte and catholyte were prepared by diluting a 1000 mg L^{-1} stock solution of sodium chloride (NaCl) to 40 mg L^{-1}, and these streams were recirculated to a single reservoir during operation.

Experimental Procedure. Experiments began by setting the flow rates of all streams: 0.2 mL min^{-1} for the feed and 1.0 mL min^{-1} for the electrode streams. These streams were transported using peristaltic pumps equipped with Tygon Chemical tubing (Saint-Gobain), and the flows were made smooth by incorporating hydraulic accumulators. The accumulators were left to pressurize the system to equilibrate overnight, after which the Gamry was set to operate at constant current. The measured voltage was allowed to stabilize for at least 1 h until it reached steady state. In all experiments, samples were collected in triplicates directly from the device in graduated cylinders and stored in centrifuge tubes for analysis, which included measurements of volume, pH, conductivity, and composition of all dissolved species. Conductivity and pH were measured using Mettler Toledo analytical instruments (SevenCompact pH/Cond S213), and composition was determined using inductively coupled plasma mass spectrometry (Agilent 7900 ICP−MS). The plasma in ICP−MS was made from argon gas and supplemented by helium, and we added an indium internal standard at 100 $\mu g\ L^{-1}$ to all samples. Quantitative analysis required calibration of the measurements, which was achieved by processing a set of reference standards and producing a calibration curve. (All standard solutions were obtained from Sigma−Aldrich.) Samples and standard solutions were diluted in 2 vol % nitric acid (HNO_3) prior to analysis by ICP−MS.

RESULTS AND DISCUSSION

To assess the ability of shock ED to separate dissolved vanadium, molybdenum, and tungsten, we used a synthetic

https://doi.org/10.1021/acs.iecr.2c02627
Ind. Eng. Chem. Res. XXXX, XXX, XXX−XXX

mixture comprising these species and varied pH. The composition of this mixture is shown in Table 2. In solution, these metals form many complexes whose distribution depends on concentration and fluid properties (e.g., pH, temperature). To define and understand possible separation schemes, we studied the speciation of vanadium, molybdenum, and tungsten using the open-source thermodynamics software DATABASE (which contains chemical reactions and equilibrium constants) and graphical user interface SPANA. With these tools, we produced chemical equilibrium diagrams of the relevant metal species in solution, as shown in Figure 2. According to these distribution diagrams, vanadium, molybdenum, and tungsten exist primarily as anionic species down to pH values of 4 (or 0 in the case of tungsten). In moderately acidic solutions ($2 < pH < 6$) and at the concentrations tested, the anionic species of vanadium include $VO_2(OH)_2^-$, $H_3V_{10}O_{28}^{3-}$, $H_2V_{10}O_{28}^{4-}$, and $HV_{10}O_{28}^{5-}$; the anionic species of molybdenum include $HMoO_4^-$, MoO_4^{2-}, $H_3Mo_7O_{24}^{3-}$, $H_2Mo_7O_{24}^{4-}$, and $HMo_7O_{24}^{5-}$; the anionic species of tungsten include WO_4^{2-} and $HW_7O_{24}^{5-}$. In strongly acidic solutions ($pH < 2$), cationic species vanadium, molybdenum, and tungsten appear and are stable: VO_2^+, MoO_2OH^+, and $H_3WO_4^+$, respectively. The distribution diagrams suggest that tungsten could be separated from vanadium and molybdenum at $pH \leq 2$ because the dominant species of the latter two metals are either neutral or cationic. Moreover, the diagrams suggest that vanadium could be separated from molybdenum at $pH \approx 2$ because the dominant species of vanadium is cationic while that of molybdenum is neutral.

In all shock ED experiments, we operated the system at constant current because it facilitates the formation of a stable deionization shock wave at overlimiting current.[23] (In contrast,

Table 2. Composition of the Feed Mixture Tested in This Study

species, j	concn, $C_0^{(j)}$	
	mg L^{-1}	mmol L^{-1}
vanadium	20	0.39
molybdenum	20	0.21
tungsten	20	0.11
sodium	42	1.8
hydronium	variable	

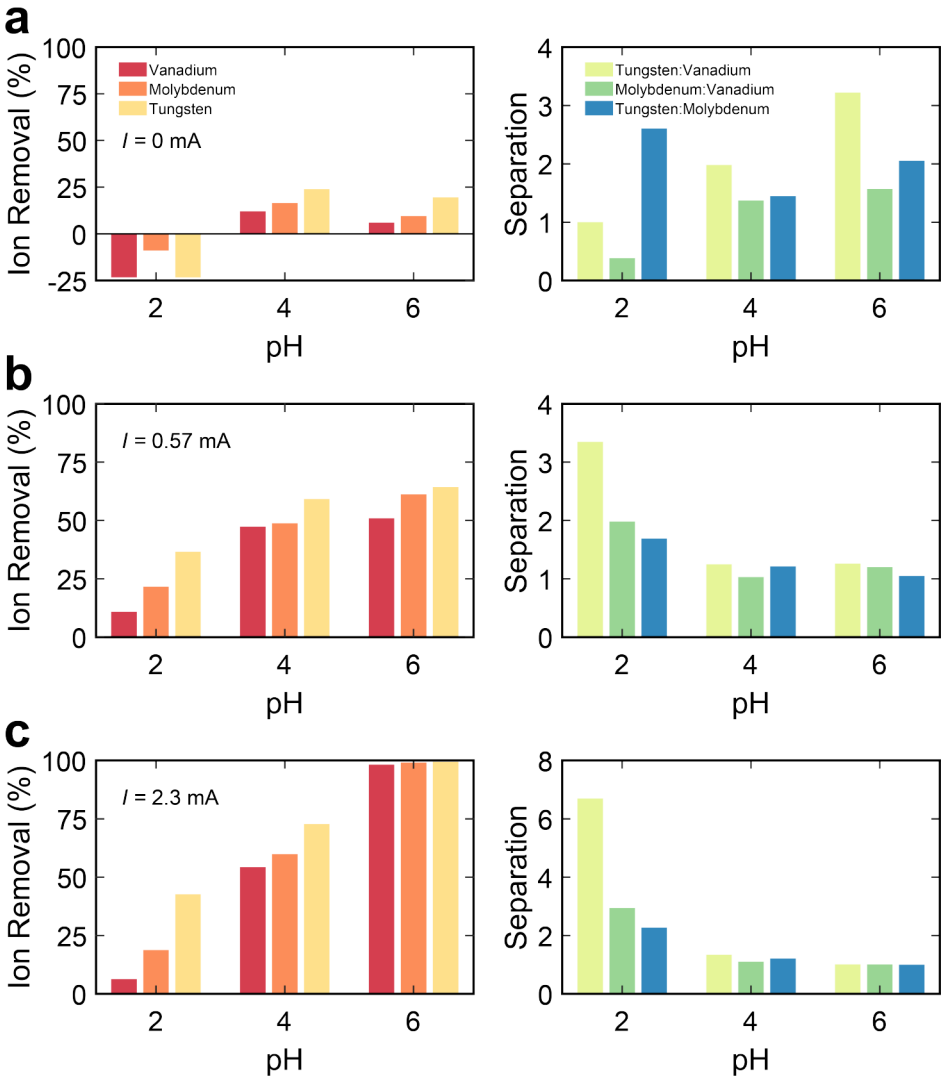

Figure 3. Quantitative analysis of selective separation of vanadium, molybdenum, and tungsten using shock ED. Ion removal (left, eq 1) and separation factor (right, eq 6) of the metals versus pH at applied currents of (a) 0 mA, (b) 0.57 mA, and (c) 2.3 mA.

https://doi.org/10.1021/acs.iecr.2c02627
Ind. Eng. Chem. Res. XXXX, XXX, XXX−XXX

operating at constant voltage can cause overshoot and oscillation about a desired overlimiting current and is associated with variability in the shock wave[40]). Our results for selective separation of vanadium, molybdenum, and tungsten are presented in Figure 3. Here, ion removal of species j in the depleted stream is defined as

$$D^{(j)} = 1 - \frac{C_D^{(j)}}{C_0^{(j)}} \tag{1}$$

enrichment of species j in the enriched stream is defined as

$$E^{(j)} = \frac{C_E^{(j)}}{C_0^{(j)}} \tag{2}$$

dimensionless current is defined as

$$\tilde{I} = \frac{I}{I_{\text{lim}}} \tag{3}$$

water recovery is defined as

$$\gamma = \frac{Q_D}{Q'} \tag{4}$$

and energy density is defined as

$$\varepsilon = \frac{IV}{Q'} \tag{5}$$

where V is (steady) voltage, and the separation factor is defined as

$$S^{(j:k)} = \frac{1 - C_D^{(j)}/C_0^{(j)}}{1 - C_D^{(k)}/C_0^{(k)}} = \frac{D^{(j)}}{D^{(k)}} \tag{6}$$

where a value of $S^{(j:k)} > 1$ suggests that species j is selectively removed relative to species k. Values of $C_0^{(j)}$ are provided in Table 2; values of $C_D^{(j)}$, $C_E^{(j)}$, $C_C^{(j)}$, and $C_A^{(j)}$ are measured experimentally. In eq 3, I is applied current, and I_{lim} is flow-limited current

$$I_{\text{lim}} = \sum_j \frac{\nu^{(j)} C_0^{(j)} F Q'}{M^{(j)}} \tag{7}$$

where ν is valence (charge), C is mass concentration, F is Faraday's constant, Q' is the volumetric flow rate of the feed, M is molar mass, and the sum is taken over all cations j (primarily sodium and hydronium). This definition of limiting current can be interpreted as the rate of forced convection of positive charge carriers into the device, and it is assumed that the flux of anions is zero at steady state in the presence of ideal cation exchange membranes.

Figure 3 shows that ion removal in the depleted stream (eq 1) generally increases with both pH and applied current, up to 99.5% at pH = 6 and I = 2.3 mA ($\tilde{I}$ = 4). We note that dimensionless current (eq 3)—a proxy for the extent of development of the deionization shock wave—depends on pH, particularly in strongly acidic solutions, as the major contributor to the limiting current (eq 7) at low pH is hydronium. For example, the concentration of hydronium at pH = 2 is 10 mmol L^{-1}, which is much greater than the concentration of sodium in our feed mixture. Moreover, a low pH reduces the magnitude of the zeta potential—a measure of the effective electric surface charge—of borosilicate glass,[41,42] which in turn decreases the extent of development of the deionization shock wave in our system.[22,30] Figure 3 also shows that the separation factor decreases with increasing pH, which reflects the fact that vanadium, molybdenum, and tungsten exist exclusively as anionic species at moderate to high pH values (see Figure 2). As a result, we expect these species to be removed to a similar extent that depends on the dimensionless current. At low pH, however, we observe selective separation of tungsten relative to vanadium and, to a lesser extent, molybdenum. This separation factor increases with applied current, which we attribute to the formation of a more developed deionization shock that promotes the mechanisms of ion selectivity in shock ED.[39] We note that pH may be decreased further to achieve greater ion separation, for example by transporting vanadium and molybdenum cations to the catholyte and accumulating tungsten oxyanions in the enriched product stream. If the system is to be operated near or above limiting current, however, the high concentration of hydronium at low pH would lower overall ion removal and significantly increase electrical energy consumption, as shown in Table 3 (we note that I_{lim} = 32 mA at pH = 1). In practice, it may be possible to achieve greater separation of a specific species at favorable conditions (i.e., high ion removal, high water recovery, low energy consumption) by using a multistage shock ED process, as we demonstrated in previous work for continuous separation of radionuclides from contaminated water.[23]

Table 3. Energy Consumption and Water Recovery Data

pH	I_{lim} (mA)	voltage (V)	energy density (kWh m^{-3})	water recovery (%)
		I = 0 mA		
2	3.7	0	0	49
4	0.60	0	0	51
6	0.57	0	0	52
		I = 0.57 mA		
2	3.7	2.6	0.13	52
4	0.60	8.5	0.41	50
6	0.57	9.1	0.44	60
		I = 2.3 mA		
2	3.7	5.6	1.1	51
4	0.60	14	2.7	56
6	0.57	19	3.8	84

In a real process, leach liquors produced from spent catalysts typically comprise several heavy metals other than vanadium, molybdenum, and tungsten. Examples of these metals include cobalt and nickel, both of which form water-stable divalent cations in acidic media. Here, we test the applicability of shock ED to first extract and then separate vanadium, molybdenum, and tungsten from a synthetic leach liquor (Table 2) that contains cobalt and nickel as well, both present at 20 mg L^{-1} (or 0.34 mmol L^{-1}). In this experiment, the solution was held at pH = 6 to ensure that vanadium, molybdenum, and tungsten were present as oxyanions that could be separated from the cations. Moreover, the anolyte and catholyte were recirculated to separate reservoirs during operation, where the catholyte was held at pH = 3. Figure 4a shows increasing removal of all species in the depleted stream as a function of current, with the greatest preference for the divalent cations, followed by sodium and then the oxyanions. In shock ED, multivalent cations tend to accumulate in the catholyte,[26,39] whereas anions accumulate in the enriched stream near the cation exchange membrane.

https://doi.org/10.1021/acs.iecr.2c02627
Ind. Eng. Chem. Res. XXXX, XXX, XXX−XXX

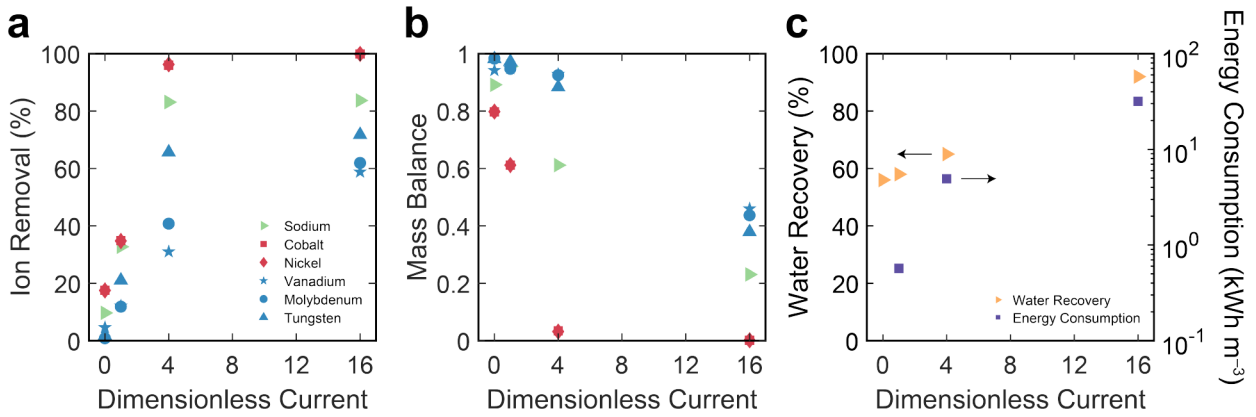

Figure 4. Quantitative analysis of selective separation of cations from anions in a synthetic leach liquor using shock ED. (a) Ion removal and (b) mass balance of the metals versus dimensionless current. (c) Water recovery and energy consumption versus dimensionless current. The synthetic leach liquor is prepared using the composition in Table 2 with 20 mg L^{-1} of both cobalt and nickel; this mixture has a limiting current of 1.0 mA at the tested flow rate.

This fractionation of oppositely charged species is captured by the mass balance in Figure 4b, which is defined as the fraction of ions fed that are retained in the main compartment of the device

$$\mu^{(j)} = \gamma \frac{C_D^{(j)}}{C_0^{(j)}} + (1-\gamma)\frac{C_E^{(j)}}{C_0^{(j)}} \tag{8}$$

These results, particularly at a dimensionless current of four, show that cobalt and nickel can be separated almost entirely in a first extraction step from vanadium, molybdenum, and tungsten, which can subsequently be separated from one another in a second purification step. In practice, cobalt and nickel can be further refined starting with the enriched catholyte produced by shock ED and using a chelating agent for speciation control, or alternatively these metals can be coprecipitated using sodium hydroxide (NaOH) to directly produce active cathode materials for batteries.

CONCLUSIONS

In summary, we successfully demonstrated the ability of shock ED, with speciation control, to continuously and selectively separate heavy metals from a multicomponent mixture that resembles the leach liquor of spent catalysts. Operation at or near neutral pH allows heavy metals such as vanadium, molybdenum, and tungsten to exist primarily as multivalent oxyanions, while other elements such as cobalt and nickel exist primarily as divalent cations. Under these conditions, the oxyanions can be separated almost entirely from the cations, with separation factors over 10, by selectively enriching the latter in the catholyte. Operation at acidic pH causes vanadium, molybdenum, and tungsten to form extensive families of oxyanions, which can then be separated from one another by up to a factor of 6 and with low energy consumption ($\leq$1 kWh m^{-3}) in a second step. We envision that the recovered cobalt and nickel can be further refined, starting with the enriched catholyte produced by shock ED, and then revalorized as precursors for the fabrication of new catalysts or battery-active materials. Similarly, the separated streams of vanadium, molybdenum, and tungsten can be further processed, and the metals can be extracted via chemical precipitation. In the future, we expect our findings on selective ion separations using shock ED to not only enable precision for targeted metal separations but also offer energy-efficient and sustainable pathways for process intensification and reduced chemical use which could improve process economics in the chemical manufacturing industry.

AUTHOR INFORMATION

Corresponding Author

Martin Z. Bazant − *Department of Chemical Engineering, Massachusetts Institute of Technology, Cambridge, Massachusetts 02139, United States; Department of Mathematics, Massachusetts Institute of Technology, Cambridge, Massachusetts 02139, United States;* orcid.org/0000-0002-8200-4501; Email: bazant@mit.edu

Author

Mohammad A. Alkhadra − *Department of Chemical Engineering, Massachusetts Institute of Technology, Cambridge, Massachusetts 02139, United States;* orcid.org/0000-0003-3866-709X

Complete contact information is available at: https://pubs.acs.org/10.1021/acs.iecr.2c02627

Notes

The authors declare no competing financial interest.

ACKNOWLEDGMENTS

The authors thank the Center for Environmental Health Sciences (CEHS) at MIT for use of ICP−MS.

REFERENCES

(1) Emsley, J.*Nature's building blocks: an AZ. guide to the elements*; Oxford University Press: 2011.

(2) Cotton, F. A.; Wilkinson, G.; Murillo, C. A.; Bochmann, M.*Advanced inorganic chemistry*; John Wiley and Sons, Inc.: 1999.

(3) Nguyen, T. H.; Lee, M. S. A review on the separation of molybdenum, tungsten, and vanadium from leach liquors of diverse resources by solvent extraction. *Geosystem Engineering* **2016**, *19*, 247−259.

(4) Saleh, T. A. Protocols for synthesis of nanomaterials, polymers, and green materials as adsorbents for water treatment technologies. *Environmental Technology & Innovation* **2021**, *24*, 101821.

(5) Saleh, T. A.; Mustaqeem, M.; Khaled, M. Water treatment technologies in removing heavy metal ions from wastewater: A review. *Environmental NanotechnologyMonitoring & Management* **2022**, *17*, 100617.

(6) Sharif, A.; Mustaqeem, M.; Saleh, T. A.; ur Rehman, A.; Ahmad, M.; Warsi, M. F. Synthesis, structural and dielectric properties of Mg/Zn ferrites-PVA nanocomposites. *Materials Science and Engineering: B* **2022**, *280*, 115689.
(7) Zeng, L.; Cheng, C. Y. A literature review of the recovery of molybdenum and vanadium from spent hydrodesulphurisation catalysts: Part I: Metallurgical processes. *Hydrometallurgy* **2009**, *98*, 1−9.
(8) Zeng, L.; Cheng, C. Y. A literature review of the recovery of molybdenum and vanadium from spent hydrodesulphurisation catalysts: Part II: Separation and purification. *Hydrometallurgy* **2009**, *98*, 10−20.
(9) Akcil, A.; Vegliò, F.; Ferella, F.; Okudan, M. D.; Tuncuk, A. A review of metal recovery from spent petroleum catalysts and ash. *Waste management* **2015**, *45*, 420−433.
(10) Park, K. H.; Reddy, B. R.; Mohapatra, D.; Nam, C.-W. Hydrometallurgical processing and recovery of molybdenum trioxide from spent catalyst. *Int. J. Miner. Process.* **2006**, *80*, 261−265.
(11) Cibati, A.; Cheng, K. Y.; Morris, C.; Ginige, M. P.; Sahinkaya, E.; Pagnanelli, F.; Kaksonen, A. H. Selective precipitation of metals from synthetic spent refinery catalyst leach liquor with biogenic H2S produced in a lactate-fed anaerobic baffled reactor. *Hydrometallurgy* **2013**, *139*, 154−161.
(12) Sigworth, E.*Potentialities of activated carbon in the metallurgical field*; American Institute of Mining, Metallurgical and Petroleum Engineers: 1962.
(13) Park, K. H.; Mohapatra, D.; Reddy, B. R. Selective recovery of molybdenum from spent HDS catalyst using oxidative soda ash leach/carbon adsorption method. *Journal of hazardous materials* **2006**, *138*, 311−316.
(14) Henry, P.; Van Lierde, A. Selective separation of vanadium from molybdenum by electrochemical ion exchange. *Hydrometallurgy* **1998**, *48*, 73−81.
(15) Nguyen, T. H.; Lee, M. S. Separation of molybdenum and vanadium from acid solutions by ion exchange. *Hydrometallurgy* **2013**, *136*, 65−70.
(16) Olazabal, M.; Orive, M.; Fernandez, L.; Madariaga, J. Selective extraction of vanadium (V) from solutions containing molybdenum (VI) by ammonium salts dissolved in toluene. *Solvent Extr. Ion Exch.* **1992**, *10*, 623−635.
(17) Nguyen, T. H.; Lee, M. S. Separation of vanadium and tungsten from sodium molybdate solution by solvent extraction. *Ind. Eng. Chem. Res.* **2014**, *53*, 8608−8614.
(18) Truong, H. T.; Kim, Y. H.; Lee, M. S. Solvent Extraction of Tungsten (VI) from Moderate Hydrochloric Acid Solutions with LIX 63. Korean. *Journal of Metals and Materials* **2017**, *55*, 405−411.
(19) Truong, H. T.; Nguyen, T. H.; Lee, M. S. Separation of molybdenum (VI), rhenium (VII), tungsten (VI), and vanadium (V) by solvent extraction. *Hydrometallurgy* **2017**, *171*, 298−305.
(20) Pan, Y.; Sun, X.; Zhang, Y. Separation of vanadium and molybdenum from aqueous solution using PEG2000+ sodium sulfate + water aqueous two-phase system. *SN Applied Sciences* **2019**, *1*, 1461.
(21) Ohto, K.; Furugou, H.; Morisada, S.; Kawakita, H.; Isono, K.-i.; Inoue, K. Stepwise Recovery of Molybdenum, Vanadium, and Tungsten with Amino-Type "Trident" Molecule by Stripping. *Solvent Extr. Ion Exch.* **2021**, *39*, 512−532.
(22) Schlumpberger, S.; Lu, N. B.; Suss, M. E.; Bazant, M. Z. Scalable and Continuous Water Deionization by Shock Electrodialysis. *Environmental Science & Technology Letters* **2015**, *2*, 367−372.
(23) Alkhadra, M. A.; Conforti, K. M.; Gao, T.; Tian, H.; Bazant, M. Z. Continuous Separation of Radionuclides from Contaminated Water by Shock Electrodialysis. *Environ. Sci. Technol.* **2020**, *54*, 527−536.
(24) Alkhadra, M. A.; Gao, T.; Conforti, K. M.; Tian, H.; Bazant, M. Z. Small-scale desalination of seawater by shock electrodialysis. *Desalination* **2020**, *476*, 114219.
(25) Conforti, K. M.; Bazant, M. Z. Continuous ion-selective separations by shock electrodialysis. *AIChE J.* **2020**, *66*, e16751.
(26) Tian, H.; Alkhadra, M. A.; Conforti, K. M.; Bazant, M. Z. Continuous and Selective Removal of Lead from Drinking Water by Shock Electrodialysis. *ACS ES&T Water* **2021**, *1*, 2269−2274.
(27) Alkhadra, M. A. Electrochemical Methods for Water Purification, Ion Separations, and Energy Conversion. *Chem. Rev.* **2022**, *122*, 13547.
(28) Alkhadra, M. A.; Jordan, M. L.; Tian, H.; Arges, C. G.; Bazant, M. Z. Selective and chemical-free removal of toxic heavy metal cations from water using shock ion extraction. *Environ. Sci. Technol.* **2022**, *56*, 14091.
(29) Dydek, E. V.; Zaltzman, B.; Rubinstein, I.; Deng, D.; Mani, A.; Bazant, M. Z. Overlimiting current in a microchannel. *Physical review letters* **2011**, *107*, 118301.
(30) Deng, D.; Dydek, E. V.; Han, J.-H.; Schlumpberger, S.; Mani, A.; Zaltzman, B.; Bazant, M. Z. Overlimiting current and shock electrodialysis in porous media. *Langmuir* **2013**, *29*, 16167−16177.
(31) Han, J.-H.; Khoo, E.; Bai, P.; Bazant, M. Z. Over-limiting current and control of dendritic growth by surface conduction in nanopores. *Sci. Rep.* **2015**, *4*, 7056.
(32) Han, J.-H.; Wang, M.; Bai, P.; Brushett, F. R.; Bazant, M. Z. Dendrite suppression by shock electrodeposition in charged porous media. *Sci. Rep.* **2016**, *6*, 28054.
(33) Mani, A.; Bazant, M. Z. Deionization shocks in microstructures. *Phys. Rev. E* **2011**, *84*, 061504.
(34) Dydek, E. V.; Bazant, M. Z. Nonlinear dynamics of ion concentration polarization in porous media: The leaky membrane model. *AIChE J.* **2013**, *59*, 3539−3555.
(35) Bazant, M. Z., Dydek, E. V., Deng, D., Mani, A.Method and apparatus for desalination and purification. 2014; US Patent US 8,801,910.
(36) National Institute of Standards and Technology (NIST), *Critically Selected Stability Constants of Metal Complexes*; 2004. https://data.nist.gov/od/id/mds2-2154 (accessed 2022).
(37) Bard, A. J.; Parsons, R.; Jordan, J.*Standard potentials in aqueous solution*; CRC Press: 1985; DOI: 10.1201/9780203738764.
(38) Cruywagen, J.*Advances in inorganic chemistry*; Elsevier: 1999; Vol. *49*, pp 127−182.
(39) Tian, H.; Alkhadra, M. A.; Bazant, M. Z. Theory of shock electrodialysis II: Mechanisms of selective ion removal. *J. Colloid Interface Sci.* **2021**, *589*, 616−621.
(40) Zangle, T. A.; Mani, A.; Santiago, J. G. On the propagation of concentration polarization from microchannel- nanochannel interfaces Part II: numerical and experimental study. *Langmuir* **2009**, *25*, 3909−3916.
(41) Lameiras, F. S.; Souza, A. L. d.; Melo, V. A. R. d.; Nunes, E. H. M.; Braga, I. D. Measurement of the zeta potential of planar surfaces with a rotating disk. *Mater. Res.* **2008**, *11*, 217−219.
(42) Liang, L.; Wang, L.; Nguyen, A. V.; Xie, G. Heterocoagulation of alumina and quartz studied by zeta potential distribution and particle size distribution measurements. *Powder Technol.* **2017**, *309*, 1−12.

https://doi.org/10.1021/acs.iecr.2c02627
Ind. Eng. Chem. Res. XXXX, XXX, XXX−XXX